



Contents lists available at ScienceDirect

Opto-Electronics Review

journal homepage: <http://www.journals.elsevier.com/geo-electronics-review>

Real time phase modulation measurements in liquid crystals

N. Bennis^{a,*}, I. Merta^a, A. Kalbarczyk^a, M. Maciejewski^b, P. Marc^a, A. Spadlo^a, L.R. Jaroszewicz^a

^a Military University of Technology, Institute of Applied Physics, ul. Kaliskiego 2, Warsaw PL-00908, Poland^b Military University of Technology, Institute of Optoelectronics, ul. Kaliskiego 2, Warsaw PL-00908, Poland

ARTICLE INFO

Article history:

Received 26 January 2017

Accepted 16 March 2017

Available online 29 April 2017

Keywords:

Young interferometer

Dynamic phase demodulation

Antiferroelectric liquid crystal

Surface electroclinic effect

ABSTRACT

We propose real time phase measurements in liquid crystals cells using Young's interferometer constructed with a new principle with possibility to control the distance between two point sources. The optical interference optical pattern is detected by a bicell photo-detector in a back Fourier focal plane. A phase modulation controlled by a monopixel liquid crystals' cell placed in a reference arm of interferometer is observed as a dynamic shift of the fringes' pattern in spatial domain. Concept of signals' demodulation in the Fourier focal plane will be described using a new approach to the demodulation signals. In this work we evaluate the demodulation condition of our setup and we present measurements of a dynamic phase response for nematic liquid crystals and antiferroelectric liquid crystals cells.

© 2017 Published by Elsevier B.V. on behalf of Association of Polish Electrical Engineers (SEP).

1. Introduction

For many applications in a bio analysis, there is a need to use a non-contact method such as interferometry, because of the object damage risk. Interferometry techniques such as laser Doppler perfusion imaging [1], electronic speckle pattern interferometer [2], scanning electronic speckle pattern interferometry [3] are successfully used for a number of medical diagnostics, including diseases of the blood and organ transplants. In this case the real time analysis of fringe patterns could limit the examination of the object under study. In the literature several works analyze the changes in the fringe pattern comparing images obtained from a CCD camera. In this case a usual process of phase extraction needs to be additionally calculated [4]. Therefore, these methods are slow and cannot accurately measure fast changes in the object under study. Phase measurements in time domain may overcome this problem and give the possibility to analyze dynamic changes of the analyzed specimen in real time. When the two wave's signals arrive at the detector plan with a different relative phase delay, results that the fringes are spatially moved through a detector or camera positioned at the Fourier plan. If the phase difference is varying very fast with time, the acquisition must be done with a high precision in time domain. In this case we are confronted with a technology problem because camera based interferometry has a limited capturing rate and long processing time for fringe pattern. On the other

hand, detector-based interferometry techniques have enough sampling rate along the time axis, but only one measurement point in spatial domain can be performed [5]. Since the phase shifts take place in space instead of time, the problem can be solved if we develop a technology taking advantage of a spatial domain control of fringe pattern. Two photo detectors placed in Fourier plane can be considered as a useful alternative when a dynamic phase is being investigated; In this case, all the data needed to calculate a phase shifting are acquired at the same time. In the present work, we adopt the basic concept Young's double slits experiments to measure the dynamic phase response, considering the possibility to optimize stable modulation conditions. This technique has been used for measuring a real-time phase modulation in nematic and antiferroelectric liquid crystals.

2. Experimental setup

The optical setup we have used to produce a double-slit Young's interferometer with a possibility to control the distance between the two point sources consists of light source coming from the laser He-Ne (632.8 nm) and passing through the polarizer Pol₁, the light was spatially filtered and collimated using lens (L₁). Then, the light was divided into two parts by a beam splitter (BS₁). One of the beams is reflected by a mirror (M₁) to act as a reference beam. The other is reflected by a second mirror (M₂) to act as a probe beam. In order to convert a large diameter collimated beam to a small diameter collimated beam, we insert a telescope formed by two positive lenses' combination in the path of reference and probe beams. Finally, the diameters of the two beams were adjusted to

* Corresponding author.

E-mail address: noureddine.bennis@wat.edu.pl (N. Bennis).

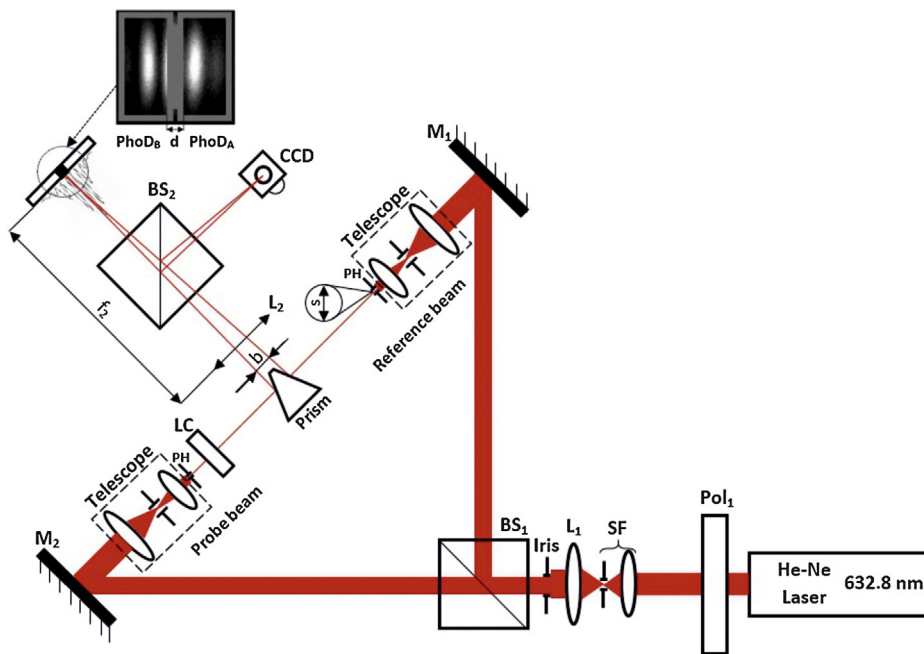


Fig. 1. Sketch of the optical setup we have used to produce a double-slit Young's interferometer with a varying distance between the source beams. Light source: HeNe laser $\lambda = 633 \text{ nm}$; Pol₁: linear polarizers; BS₁ and BS₂: beam splitters; M₁ and M₂: mirrors; PH: pinhole; LC: liquid crystal cell; L₁, L₂: lenses.

the size (s of 400 μm). This tiny collimated beam spot size has been established, when circular pinhole (PH) with a diameter of 400 μm is inserted in the path of beams. As a result the output beams of a diameter of 400 μm with a homogeneous distribution of amplitude and phase is obtained. This parameter determines the distribution envelope of the interference pattern. A gold coated right angle prism mirror has been used to bend light coming out from pinholes by 90 degrees. Therefore, the reflected rays from both sides of the prism become parallel to each other separated by the distance b (Fig. 1). The two beams are combined by Fourier Lens (L₂) and the interference pattern is observed at the focal plane of lens L₂, where two photo-detectors PhoD_A and PhoD_B separated from each other by the distance gap d (Fig. 1) are located. In order to conduct an appropriate fringe pattern, it is necessary to make both beams focus at the same point. Accordingly second BS₂ has been used to monitor a focused image of each point source in a CCD camera and to allow the fringe pattern to be viewed.

We have used photo detectors with an active area of 2.5 mm \times 2.5 mm, segmented into two cells with a 48 μm gap. In Fourier plane, the size of airy disc containing fringe pattern is determined by the source size s of interfering beams, the wavelength λ and the focal length f . These parameters have been chosen to fix the Airy disc to approximately 500 μm diameter size. The advantage of this arrangement setup consists of spatial domain control of the fringe pattern which the period of spatial modulation of intensity distribution can be controlled varying the distance between two point sources' beams by moving the prism position. In this case, the spatial distribution of intensity will be recorded simultaneously in two photo detectors.

During the measurement the LC cell under study was placed in a probe beam inside a hot-stage maintaining a constant temperature of 35 °C.

2.1. Adjustment conditions for an optical phase demodulation

Phase demodulation performance is strongly determined by geometrical parameters of the above setup such as a distance

between two point sources and distance between two photo-detectors (see Fig. 1).

The electric signals coming out from PhoD_A and PhoD_B are collected in a data acquisition card (DAC) controlled by LabVIEW software. Those signals are added (*Sum*) and subtracted (*Diff*) to each other:

$$\begin{aligned} \text{Sum} &= I_A + I_B \\ \text{Diff} &= I_A - I_B \end{aligned} \quad (1)$$

Information about a phase shift in the observed fringe pattern can be described by using *Sum* and *Diff* characteristics described in reference [6]:

$$\begin{aligned} \text{Sum} &= 2a_1 + 2a_2 \cos \Delta\varphi \\ \text{Diff} &= 2a_3 \sin \Delta\varphi \end{aligned} \quad (2)$$

where a_1 , a_2 and a_3 depend on the wavelength λ , the focal length f , the distance between the two point sources b and the beam size s . Those parameters can be given as integral of interference pattern over receiving area of photo-detectors, such as:

$$\begin{aligned} a_1 &= C \int_{d/2}^{\infty} \int_{-\infty}^{\infty} A^2(\rho) dy_f dx_f \\ a_2 &= C \int_{d/2}^{\infty} \int_{-\infty}^{\infty} A^2(\rho) \cos \left(\frac{4\pi b x_f}{\lambda f} \right) dy_f dx_f \\ a_3 &= C \int_{d/2}^{\infty} \int_{-\infty}^{\infty} A^2(\rho) \sin \left(\frac{4\pi b x_f}{\lambda f} \right) dy_f dx_f \end{aligned} \quad (3)$$

where $A(\rho)$ is the spatial distribution of amplitude on the Fourier plane. For the uniform input beam this distribution is expressed as:

$$A(\rho) = \left(\frac{2J_1(\pi\rho s)}{\pi\rho s} \right) \quad (4)$$

where J_1 is the Bessel function of the first-order and ρ represents the radius in the spatial frequency domain [7].

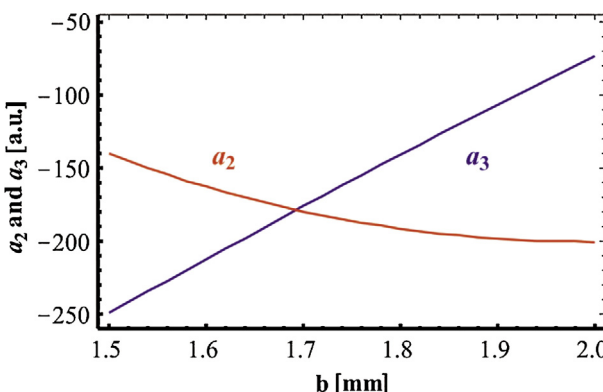


Fig. 2. Evolution of a_2 and a_3 as a function of b . Parameters of this simulation are: $s = 400 \mu\text{m}$, $\lambda = 0.633 \mu\text{m}$, $f = 170 \text{ mm}$ and $d = 48 \mu\text{m}$.

Detailed procedure for phase shift measurements' certitude using this method is described in Ref. [6]:

$$\Delta\phi = \tan^{-1} \left[\frac{(I_A - I_B)a_2}{a_3(I_A + I_B) - 2a_1} \right] \quad (5)$$

The parameter a_1 can be omitted by blocking data DC offset removal from input signals using AC coupling in Digital Acquisition Cards. It is necessary to obtain equality between a_2 and a_3 . In this case, the linear relation between the optical phase and the photodetector output can be obtained by:

$$\Delta\phi = \tan^{-1} \left[\frac{I_A - I_B}{I_A + I_B} \right] \quad (6)$$

Fig. 2 shows a numerical simulation plot of a_2 and a_3 as a function of b , considering a finite source size ($s = 400 \mu\text{m}$) of interfering beams, wavelength ($\lambda = 0.633 \mu\text{m}$), focal length ($f = 175 \text{ mm}$) and distance between the two point sources ($d = 48 \mu\text{m}$). These parameters have impact on size of an airy disc in Fourier plane. The distance between two point sources was varied over an interval between 1.5 mm and 2 mm.

Those results indicate that, the values of a_2 and a_3 depend strongly on two point sources separation. The proper selection to obtain the condition of $a_2 = a_3$ is when spacing between two point sources is of about 1.7 mm. In this case the maximum number of interference fringes that could be viewed is seven which give rise to a fringe separation of $81.6 \mu\text{m}$ [see Fig. 3(a)]. Based on this simulation results, the experimental fringe pattern was captured by the CCD image sensor at the focal plane varying the prism position. The optimal choice to calculate the phase shift directly from Eq. (6) can be established when the prism position corresponds to display seven interference fringes on CCD camera (see Fig. 3(b)).

Simple mathematical operations such as addition and subtraction of the intensity recorded by each photo-detector allow for a dynamic phase shift to be directly evaluated.

3. Dynamic phase measurement in a nematic liquid crystal cell

For pure phase modulation measurement, 5 μm -thick cells have been fabricated, employing SE-130 as an alignment layer for a homogeneous orientation. The cell is antiparallel rubbed, which provides uniform alignment, and filled with a Merck liquid crystal E7, having a birefringence of $\Delta n \approx 0.21$ at $\lambda = 632.8 \text{ nm}$.

Pure phase modulation can be obtained by aligning the optical axis of nematic liquid crystals (NLC) parallel to the linearly polarized impinging light. Applying the voltage to the cell, the refractive index may change achieving phase only modulation of the light beam, therefore we can generate the phase shifts between the ref-

erence and the objects beams while the waveform is applied to the NLC cell. Phase changes between the interfering beams can be controlled by a liquid crystal cell placed in one branch of the interferometer. Modulated waveform between two voltages values with certain modulation frequency must be applied to the cell to produce a temporal phase shift. In this work, the waveform used to switch dynamically the cell, consists of 240 Hz square signal modulated by 25 Hz square envelope [Fig. 4(a)]. The applied AC voltage to the LC was varied between 0 and 10 V. As the voltage was applied, the LC director began to realign parallel to the electric field, until the phase shift gradually reached a steady state. Once the driving voltage was removed, the molecules slowly relaxed to their initial position. After adding and subtracting the intensity signals detected by two photo-detectors [Fig. 4(b)], a dynamic phase shift is obtained from Eq. (6) gives rise to a saw-tooth function [Fig. 4(c)], showing the phase modulo 2π phase jumps. Using the phase unwrapping method this 2π phase jump can be avoided, therefore continuous function of relative phase shift is generated [Fig. 4(d)].

The time-varying phase shift of a liquid crystal cell can be directly analyzed in our measurement setup. The phase shift achieves its maximum values when the molecules have enough time to relax to their horizontal position. From these results it can be seen that the phase modulation range of almost 3.2π is obtained when the relaxation time is about 20 ms. This measurement value is rather close to the calculated total phase shifts (3.32π). From Fig. 4(d), a phase fluctuation is detected during the alternative square waveform pulses. This Phase fluctuation may affect the efficiency of a photonic device based on the liquid crystal technology; therefore, it should be taken into consideration when the phase modulation is required [8].

4. Dynamic phase switching in orthoconic antiferroelectric liquid crystals

Surface stabilized orthoconic antiferroelectric liquid crystals (OAFLC) have great potential for use in display applications [9–11], they offer the same fast switching time as ferroelctric liquid crystals, but they have advantage of three stable state and grey scale generation in display. The rod like molecules in OAFLC are arranged in layers and tilted alternatively with regard to the normal layer. In the absence of the applied voltage, the optical axis is along the normal layer. We have carried out the dynamic phase measurement to afford information regarding the dynamic switching of optical axis director in (OAFLC). The waveform applied to the cell consists of a voltage pulse of 300 μs , followed by a long reset (10 ms) to initialize the switching state from synclinic state to anticlinic state. For the proposed waveform, fast relaxation time of an OAFLC cell was found to be an issue that may be of major concern in the phase shift measurement between two consecutive frames. For this purpose we have carried out dynamic phase measurements in fast switching samples made with polymer network formed in a mixture with the direct phase transition between SmC_A^* phase and isotropic which was prepared based on compounds described in Refs. [12,13]. In situ photopolymerization method in the orthoconic antiferroelectric liquid crystal cells is described in Ref. [14]. Due to the polymer network, the relaxation time from a synclinic to anti-clinic state after switching OFF the field is reduced. Depending on the polarity of the applied electric field, two orientations of the optical axis are possible; therefore, we can switch the optical axis between three orthogonal states. In such switching, the molecules rotate in plane perpendicular to the direction of propagation of the incident light. Rotation of the molecules in such plane can provide modulation of the intensity of an incident optical field but do not provide pure phase modulation. Orthoconic liquid crystal cells (OAFLC) can afford three phase levels without coupling amplitude

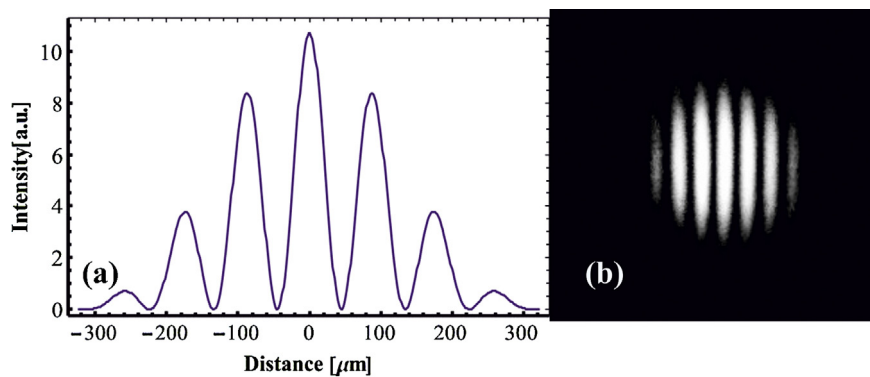


Fig. 3. (a) Simulated interference pattern corresponding to $b = 1.7$ mm. (b) The corresponding experimental interference pattern captured by CCD.

[15]. In this case the incident beam should be linearly polarized in a direction parallel to one of the switched state.

The results in Fig. 5 show that an OAFLC cell can be dynamically switched between three equidistant phase levels in the range of a 2π phase. Analyses of the phase dynamics of an OAFLC cell in time domain could provide new information that enables us to understand dynamic switching in the OAFLC cell. Fig. 5 reveals that after releasing the electric field the optical axis orientation does not return completely to an anticlinic state, indicating some kind of remanence of a ferroelectric order, in this case a synclinic state is upheld during few milliseconds which causes that the relaxation to anticlinic state becomes slower. The phenomenon which keeps

the director tilted in the absence of electric field could be related to the surface electroclinic effect in OAFLC cells observed in Ref. [16]. Note that the time remanence of ferroelectric state after relaxation from a positive voltage pulse is kept longer than other ferroelectric state corresponding to a negative voltage pulse, which indicates that the surface electroclinic effect of this cell prefers the positive voltage state, however, disfavoured the negative voltage state. In future investigations we want to focus on a possibility to develop a multilevel phase measurement in an orthoconic OAFLC in order to validate their working in photonic applications.

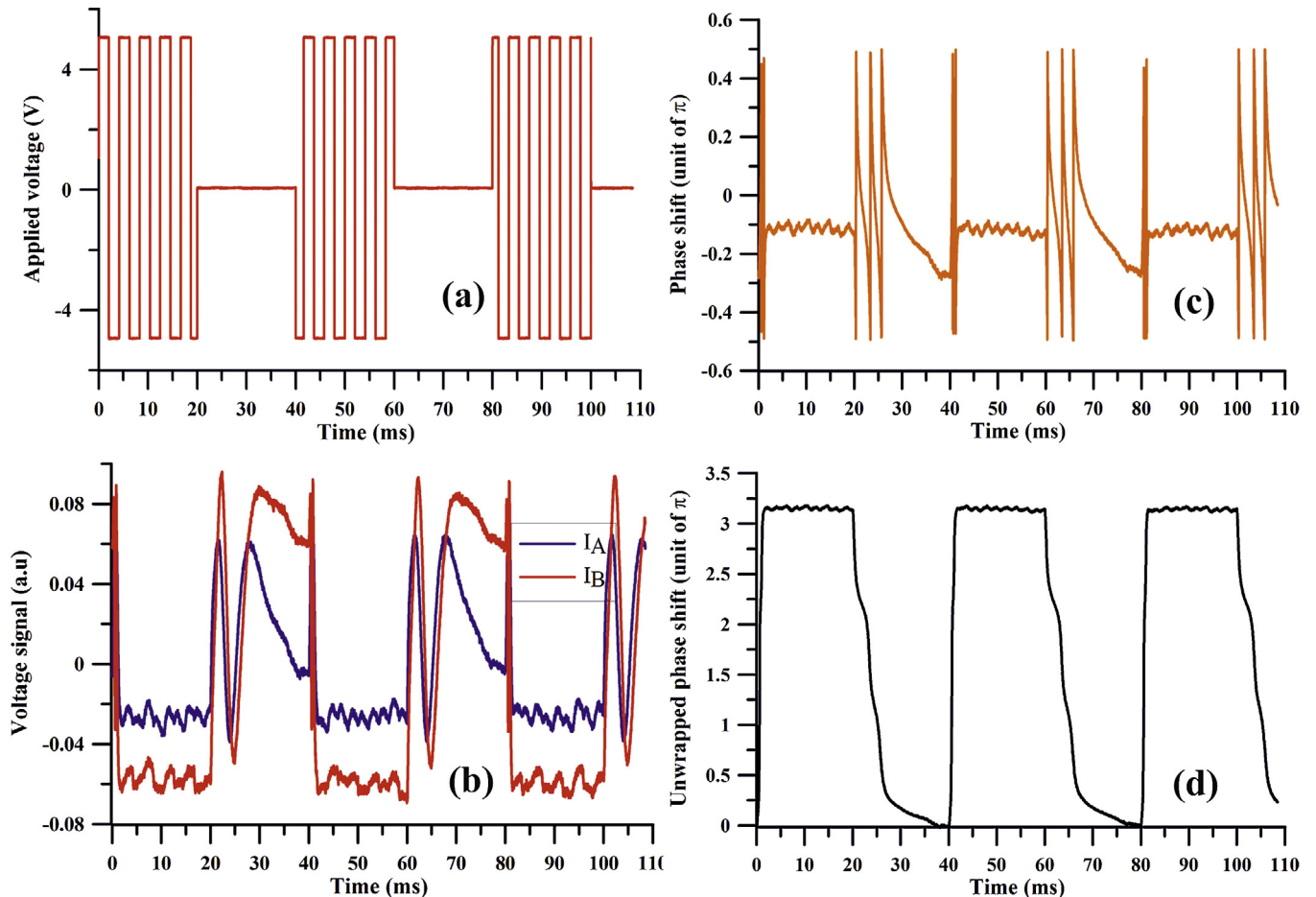


Fig. 4. Measurement procedure of dynamic phase shifts in a liquid crystal cell: (a) modulated waveform, (b) signals detected by two photo-detectors, (c) dynamic phase shift and (d) unwrapped phase shift.

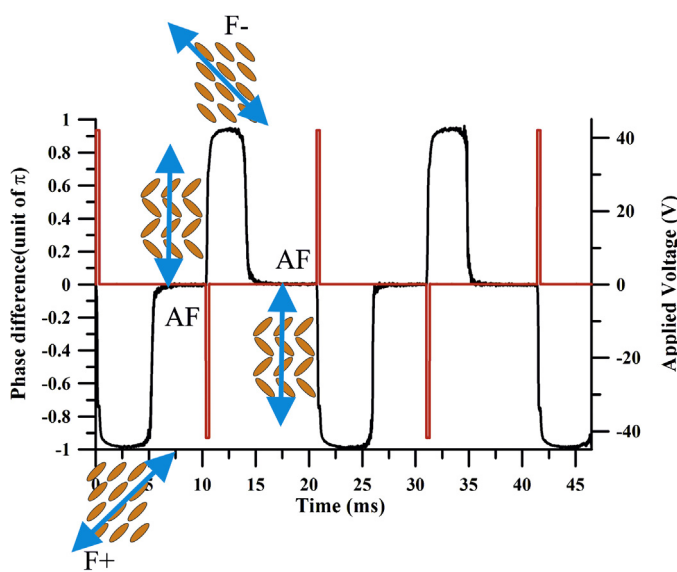


Fig. 5. Dynamic phase switching between three different extreme states in an orthoconic antiferroelectric liquid crystal: red line wave form, black line phase response.

5. Conclusions

We proposed an optical setup for dynamic phase shift measurements in liquid crystal cells; this setup enables simple and automatic measurements of the time varying phase with high sensitivity. The advantage of our demodulation technique consists of spatial domain control of a fringe pattern which the period of spatial modulation of the intensity distribution can be controlled varying the distance between two point sources of a Young's interferometer setup. The measured phase shifts as a function of time allow us to extract information about time phase fluctuations in nematic liquid crystals and dynamic of the optical axis switching in orthoconic antiferroelectric liquid crystals.

Acknowledgements

We acknowledge financial support from Polish Ministry of Science and Higher Education, the Statutory Activity PBS-654 of Military University of Technology.

References

- [1] C. Magnain, A. Castel, T. Boucneau, M. Simonutti, I. Ferezou, A. Rancillac, T. Vitalis, J.A. Sahel, M. Paques, M. Atlan, Holographic laser Doppler imaging of microvascular blood flow, *J. Opt. Soc. Am. A* 31 (12) (2014) 2723–2735.
- [2] V. Bavigadda, E. Mihaylova, R. Jallapuram, V. Toal, Vibration phase mapping using holographic optical element-based electronic speckle pattern interferometry, *Opt. Lasers Eng.* 50 (8) (2012) 1161–1167.
- [3] Pablo Ruiz, Jonathan M. Huntley, Ricky D. Wildman, Depth-resolved whole-field displacement measurement by wavelength-scanning electronic speckle pattern interferometry, *Appl. Opt.* 44 (19) (2005) 3945–3953.
- [4] R. Balamurugan, S. Muruganand, Electronic laser speckle interferometer for displacement measurement using digital image processing technique, *J. Image Graph.* 1 (1) (2013) 59–62.
- [5] Y. Fu, G. Pedrini, X. Li, Interferometric dynamic measurement: techniques based on high-speed imaging or a single photodetector, *Sci. World J.* 2014 (2014) 1–14, Article ID 232906.
- [6] I. Merta, Z. Holdynski, P. Marc, L.R. Jaroszewicz, Bicell-photodetector in the Fourier plane as a fiber optic homodyne phase demodulator: theoretical model and experimental results, *Appl. Opt.* 19 (52) (2013) 4468–4476.
- [7] J.W. Goodman, *Introduction to Fourier Optics*, 2nd ed., McGraw-Hill, New York, 1996.
- [8] A. Lizana, I. Moreno, A. Márquez, C. Iemmi, E. Fernández, J. Campos, M.J. Yzuel, Time fluctuations of the phase modulation in a liquid crystal on silicon display: characterization and effects in diffractive optics, *Opt. Exp.* 16 (21) (2008) 16711–16722.
- [9] J.M. Oton, X. Quintana, P.L. Castillo, A. Lara, V. Urruchi, N. Bennet, Antiferroelectric liquid crystal displays, *Opto Electron. Rev.* 12 (3) (2004) 263–269.
- [10] H. Takezoe, E. Gorecka, M. Čepič, Antiferroelectric liquid crystals: interplay of simplicity and complexity, *Rev. Mod. Phys.* 82 (2010) 897–937.
- [11] P. Rudquist, Orthoconic antiferroelectric liquid crystals, *Liq. Cryst.* 40 (12) (2013) 1678–1697.
- [12] K. Milewska, W. Drzewiński, M. Czerwiński, R. Dąbrowski, W. Piecik, Highly tilted liquid crystalline materials possessing a direct phase transition from antiferroelectric to isotropic phase, *Mater. Chem. Phys.* 171 (2016) 33–38.
- [13] K. Milewska, W. Drzewiński, M. Czerwiński, R. Dąbrowski, Design, synthesis and mesomorphic properties of chiral benzoates and fluorobenzoates with direct SmCA*-Iso phase transition, *Liq. Cryst.* 42 (11) (2015) 1601–1611.
- [14] P. Rudquist, D. Elfström, S.T. Lagerwall, R. Dabrowski, Polymer-stabilized orthoconic antiferroelectric liquid crystals, *Ferroelectrics* 344 (2006) 177–188.
- [15] D. Engström, P. Rudquist, J. Bengtsson, K. D'havé, S. Galt, Three-level phase modulator based on orthoconic antiferroelectric liquid crystals, *Opt. Lett.* 31 (21) (2006) 3158–3160.
- [16] R. Beccherelli, S.J. Elston, Evaluation of optical anisotropy in the pretransitional regime in antiferroelectric liquid crystals, *Liq. Cryst.* 25 (5) (1998) 573–577.